

# Hierarchical Core-Shell Structures of P-Ni(OH)<sub>2</sub> Rods@MnO<sub>2</sub> Nanosheets as High Performance Cathode Material for Asymmetric Supercapacitors

Kunzhen Li<sup>a</sup>, Shikuo Li<sup>b</sup>, Fangzhi Huang<sup>b</sup>, Xinyao Yu,<sup>c</sup> Yan Lu<sup>a</sup>, Lei  
Wang<sup>a</sup>, Hong Chen<sup>a</sup> and Hui Zhang<sup>a</sup>, \*

a. School of Physics and Materials Science, Anhui University, Hefei 230601, P. R. China

b. School of Chemistry and Chemical Engineering, Anhui University, Hefei 230601, P. R. China

c. School of Materials Science & Engineering, Zhejiang University, Hangzhou 310027, P. R. China

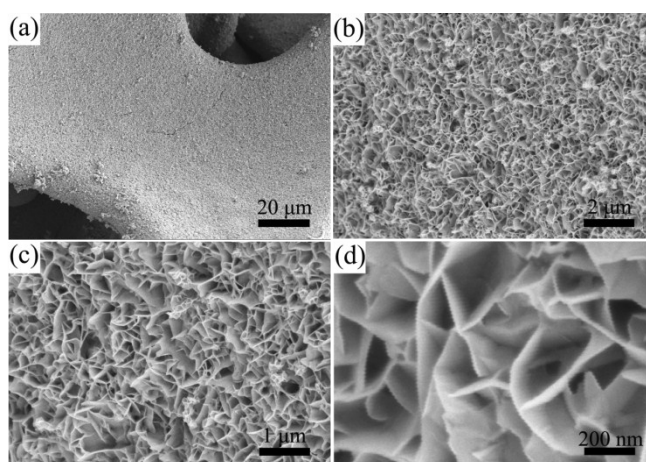


Fig.S1. SEM images (a-d) of the MnO<sub>2</sub> nanosheets grown on Ni foam at low and high magnifications.

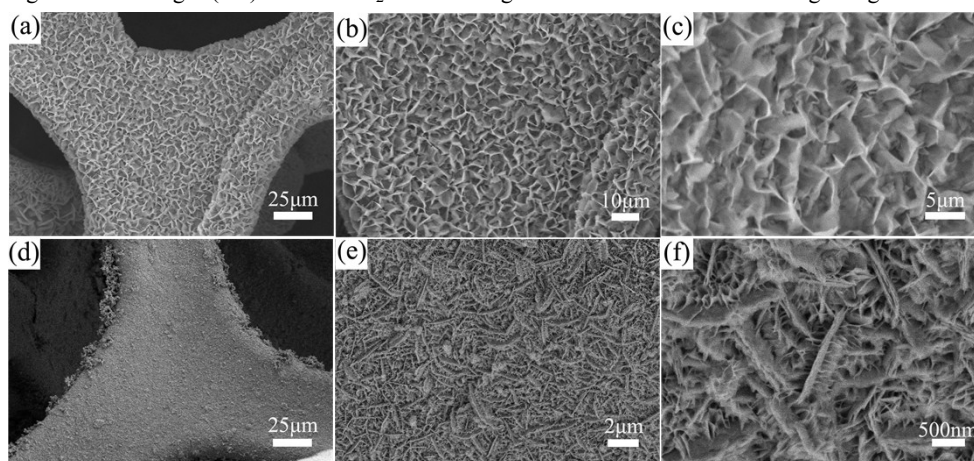


Fig.S2. SEM images of the Ni(OH)<sub>2</sub> nanosheets (a-c) and Ni(OH)<sub>2</sub>@MnO<sub>2</sub> nanosheets (d-f) grown on Ni foam at low and high magnifications.

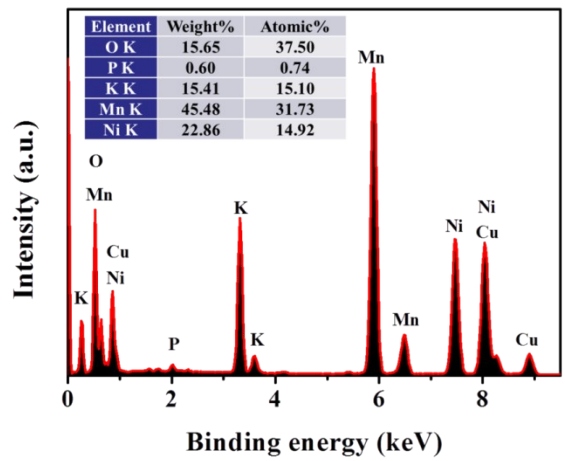


Fig.S3. TEM-EDX results for the hierarchical P-Ni(OH)<sub>2</sub>@MnO<sub>2</sub> core/shell sample.

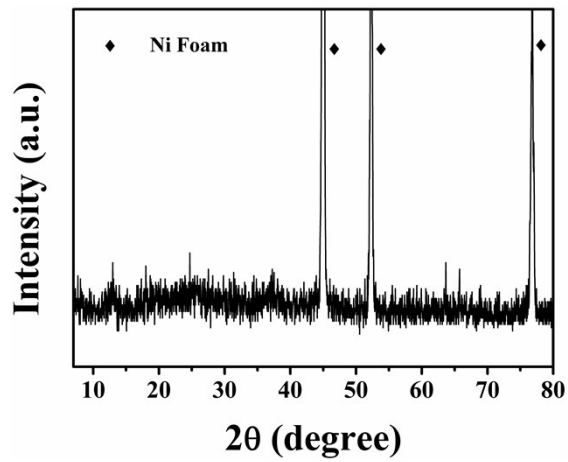


Fig.S4. XRD spectra of the hierarchical P-Ni(OH)<sub>2</sub>@MnO<sub>2</sub> core/shell nanostructures grown on Ni foam.

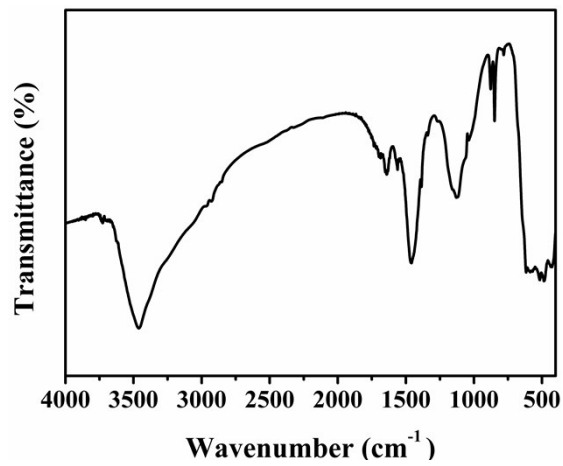


Fig.S5. FT-IR spectrum of the hierarchical P-Ni(OH)<sub>2</sub>@MnO<sub>2</sub> core/shell sample.

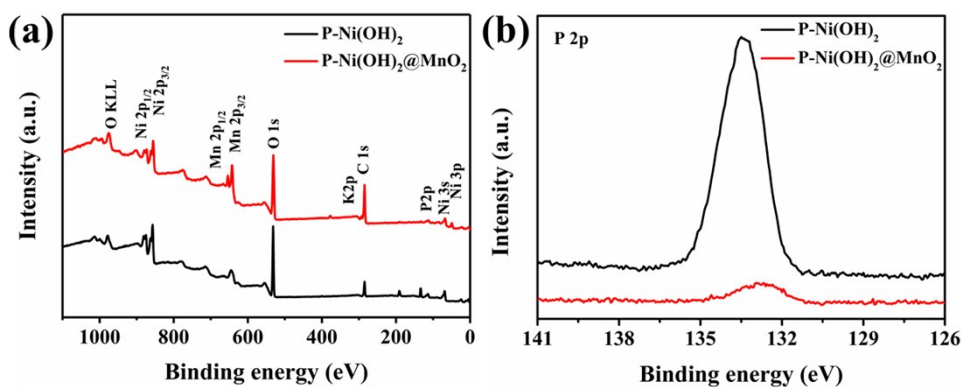


Fig. S6. (a) XPS survey spectra and (b) XPS spectra of P 2p from the pristine P-Ni(OH)<sub>2</sub> and the hierarchical P-Ni(OH)<sub>2</sub>@MnO<sub>2</sub> core/shell samples.

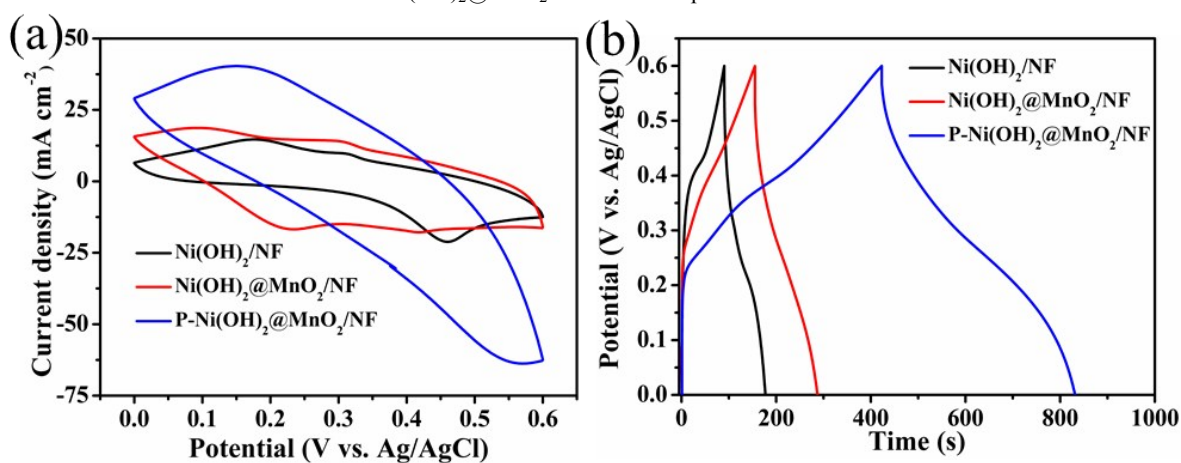


Fig.S7. (a) CV and (b) GCD curves of the Ni(OH)<sub>2</sub>/NF, Ni(OH)<sub>2</sub>@MnO<sub>2</sub>/NF and P-Ni(OH)<sub>2</sub>@MnO<sub>2</sub>/NF electrodes at 10 mVs<sup>-1</sup> and 10 mA cm<sup>-2</sup>.

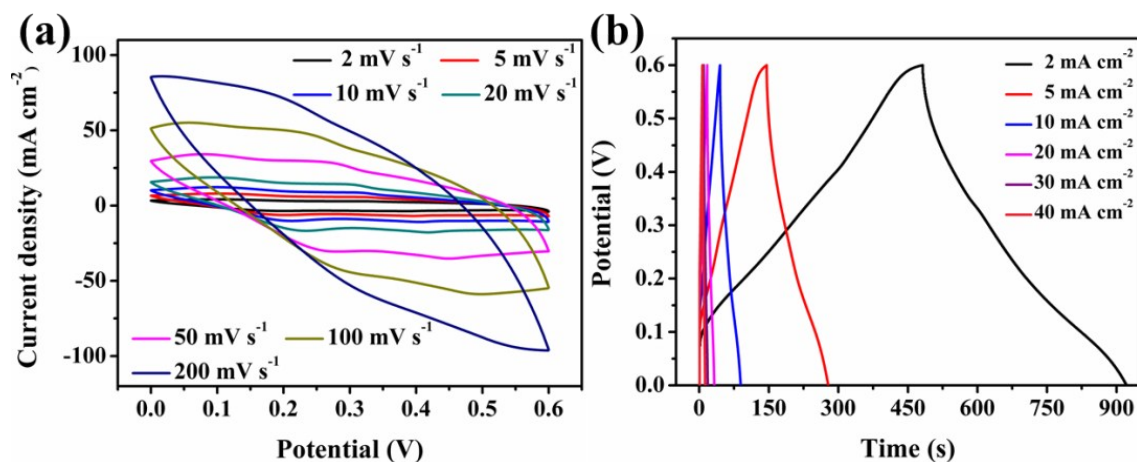


Fig.S8. (a) CV curves of the MnO<sub>2</sub>/NF electrode at different scan rates; (b) GCD curves of the MnO<sub>2</sub>/NF electrode at different current densities.

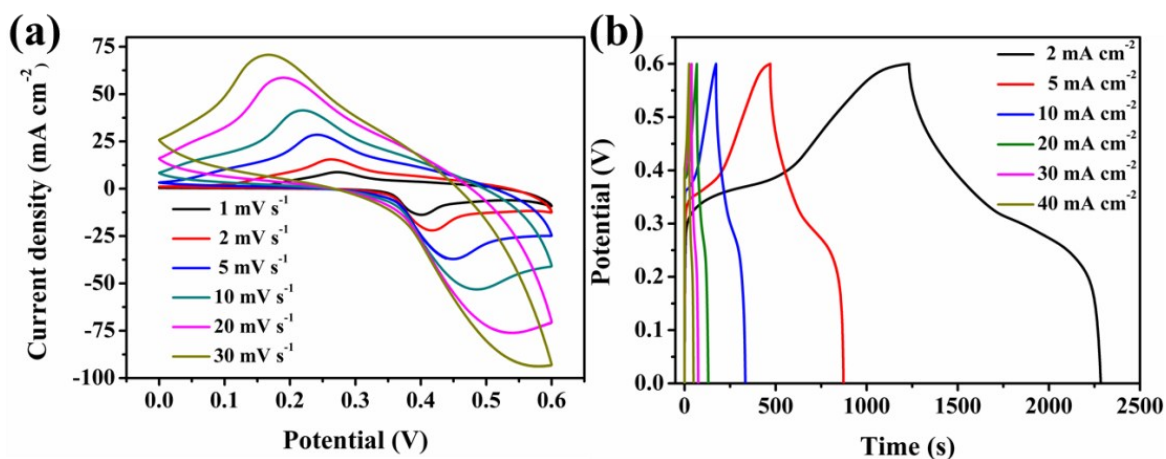


Fig.S9. (a) GCD curves of the P-Ni(OH)<sub>2</sub>/NF electrode at different scan rates; (b) GCD curves of the P-Ni(OH)<sub>2</sub>/NF electrode at different current densities.

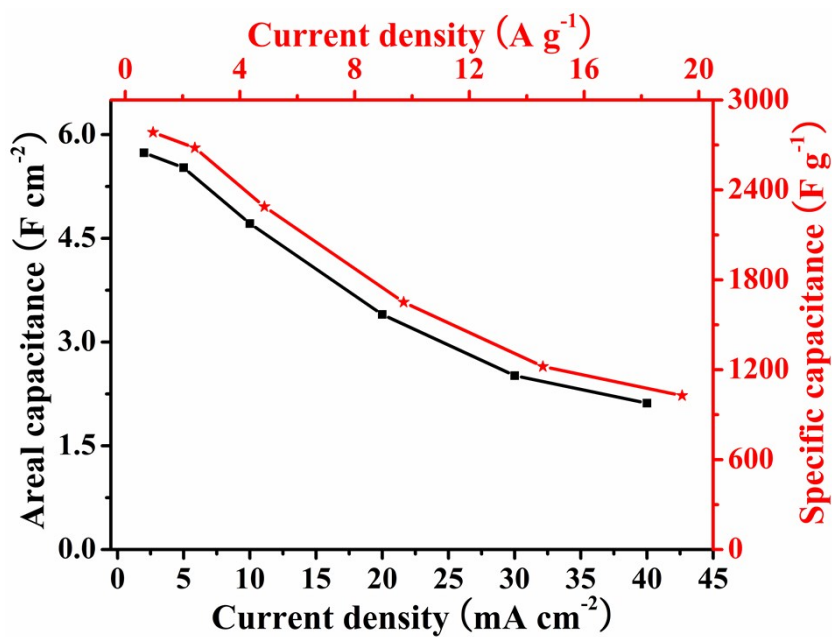


Fig.S10.The corresponding specific capacitance of the P-Ni(OH)<sub>2</sub>@MnO<sub>2</sub>/NF electrode at different current density.

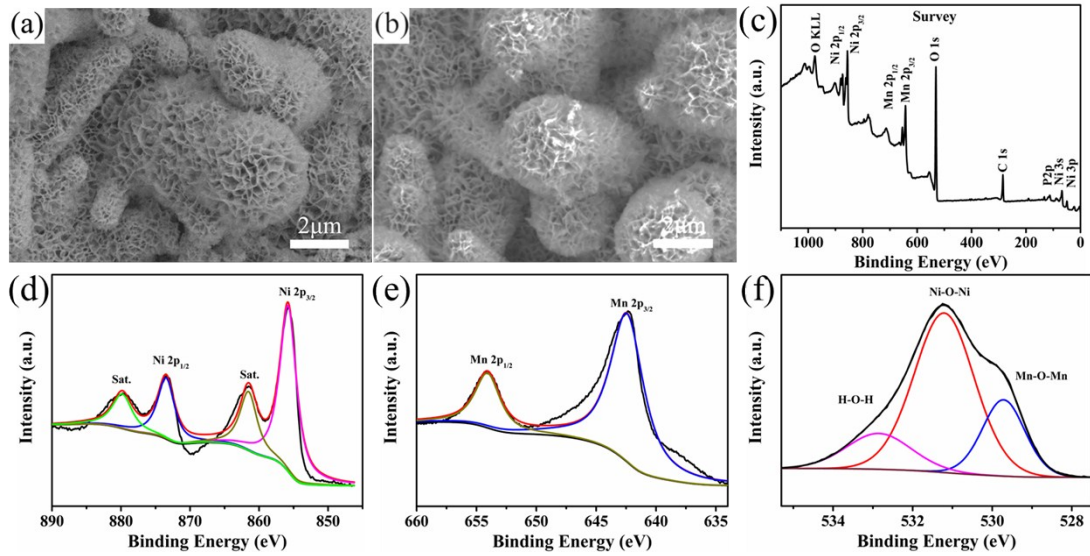


Figure S11. SEM images of typical hierarchical porous P-Ni(OH)<sub>2</sub>@MnO<sub>2</sub> core/shell nanostructure grown on 3D Ni foam electrode (a) before and (b) after cycling for 10000 cycles. XPS survey spectra of the typical P-Ni(OH)<sub>2</sub>@MnO<sub>2</sub> electrode sample after 10000 cycles (c), Ni 2p (d), Mn 2p (e) and O 1s (f).

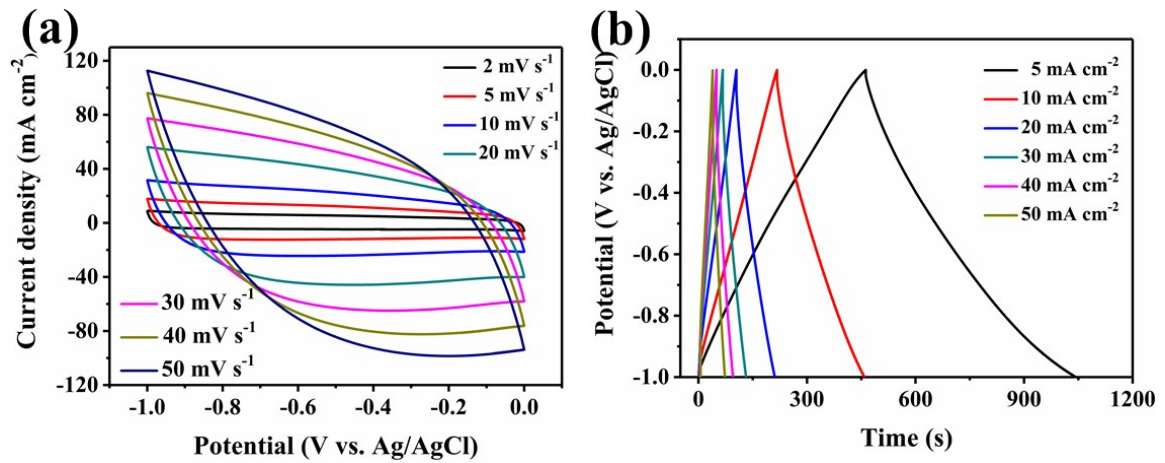


Fig.S12. (a) CV curves of the AC at different scan rates; (b) GCD curves of the AC at different current densities.

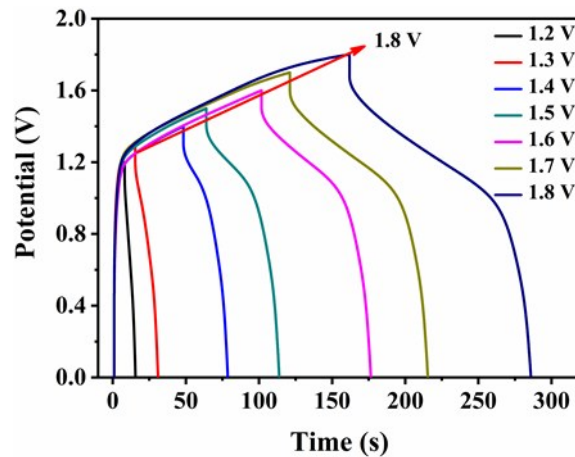


Fig.S13. GCD curves of the P-Ni(OH)<sub>2</sub>@MnO<sub>2</sub>/NF and activated carbon electrodes at different voltage window.

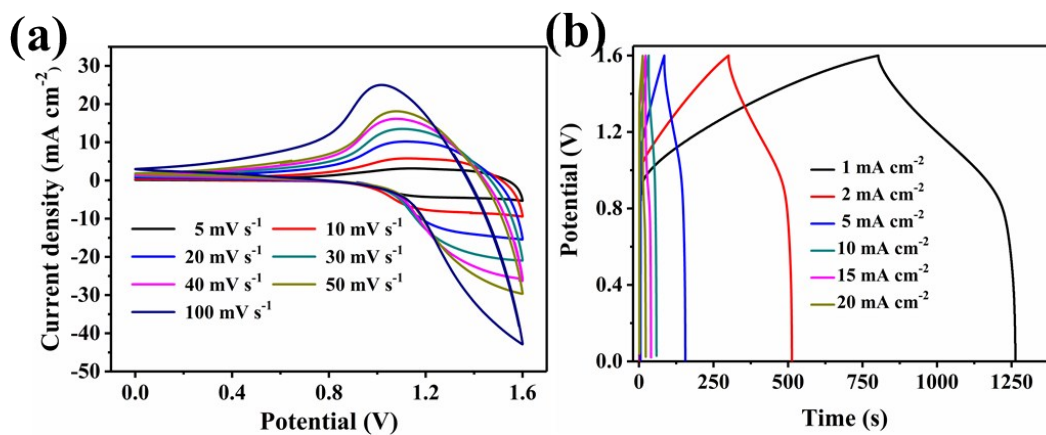


Fig.S14. (a) CV curves of the P-Ni(OH)<sub>2</sub>/NF//AC at different scan rates; (b) GCD curves of the P-Ni(OH)<sub>2</sub>/NF//AC at different current densities.

Table S1

Asymmetric supercapacitors	Electrolyte	Potential window (V)	Specific capacitance	Maximum energy density	Maximum power density	Retention(%) / cycling number / current density	Refs.
CoFe <sub>2</sub> O <sub>4</sub> @MnO <sub>2</sub> // AC	3 M KOH	1.6	0.883 F cm <sup>-2</sup>	37 Wh Kg <sup>-1</sup>	4800 W Kg <sup>-1</sup>	91.5% % after 2250 at 41 mA cm <sup>-2</sup>	<sup>1</sup>
NiCo <sub>2</sub> O <sub>4</sub> @MnO <sub>2</sub> // AC	1 M NaOH	1.5	0.52 F cm <sup>-2</sup>	35 Wh Kg <sup>-1</sup>		71% % after 5000 at 18 mA cm <sup>-2</sup>	<sup>2</sup>
Ni(OH) <sub>2</sub> /MnO <sub>2</sub> @CNT//APDC	1 M KOH	1.7	315 F g <sup>-1</sup>	10.9 mWh cm <sup>-3</sup>	424.1 mW cm <sup>-3</sup>	78.2% after 3000 at 0.5 A g <sup>-1</sup>	<sup>3</sup>
MnO <sub>2</sub> @CF//FeO OH/PPy@CF	LiCl/PVA	1.6	5.5 F cm <sup>-3</sup>	2 mWh cm <sup>-3</sup>		82% after 5000 at 100 mV s <sup>-1</sup>	<sup>4</sup>
PEDOT@MnO <sub>2</sub> /C@Fe <sub>3</sub> O <sub>4</sub>	LiCl/PVA	2	60 mF cm <sup>-2</sup>	0.0335 mWh cm <sup>-2</sup>		80% after 800 at 2 mA cm <sup>-2</sup>	<sup>5</sup>
MnO <sub>2</sub> /PEDOT: PSS/CNT//VN@C NWAs/CNT	Na <sub>2</sub> SO <sub>4</sub> /PVA	1.8	213.5 mF cm <sup>-2</sup>	96.07 μWh cm <sup>-2</sup>	2700 μW cm <sup>-2</sup>	96.8% after 5000 at 2 mA cm <sup>-2</sup>	<sup>6</sup>
MnO <sub>2</sub> /GMG//GCF	LiCl/PVA	1.6	16.8 mF cm <sup>-2</sup>	11.9 μWh cm <sup>-2</sup>		92.7% after 8000 at 1 mA cm <sup>-2</sup>	<sup>7</sup>
NPG@MnO <sub>2</sub> //CNT/CP	LiCl/PVA	1.8	12 mF cm <sup>-2</sup>	5.4 μWh cm <sup>-2</sup>	2531 μW cm <sup>-2</sup>	90% after 2000 at 0.6 mA cm <sup>-2</sup>	<sup>8</sup>
MnO <sub>2</sub> -PPy//V <sub>2</sub> O <sub>5</sub> -PANI	4 M LiCl	2	0.613 F cm <sup>-2</sup>	0.340 mWh cm <sup>-2</sup>	30 mW cm <sup>-2</sup>	almost 100 % after 5000 at 30 mA cm <sup>-2</sup>	<sup>9</sup>
rGO@ MnO <sub>2</sub> //rGO paper	1M Na <sub>2</sub> SO <sub>4</sub>	1.5	113 mF cm <sup>-2</sup>	35.1 μWh cm <sup>-2</sup>	3.8 mW cm <sup>-2</sup>	84% after 1500 at 15 mA cm <sup>-2</sup>	<sup>10</sup>
Ni(OH) <sub>2</sub> NW //Carbon fiber	KOH/PVA	1.5	35.67 mF cm <sup>-2</sup>	0.01 mWh cm <sup>-2</sup>	7.3 mW cm <sup>-2</sup>	70% after 10000 at 0.5 mA cm <sup>-2</sup>	<sup>11</sup>
Ni(OH) <sub>2</sub> -N G//NG	H <sub>2</sub> SO <sub>4</sub> /PVA	1.45	255 mF cm <sup>-2</sup>	79.5 μWh cm <sup>-2</sup>	3.9 mW cm <sup>-2</sup>	92% after 10000 at 4 mA cm <sup>-2</sup>	<sup>12</sup>
P-Ni(OH) <sub>2</sub> @MnO <sub>2</sub> /NF//AC	LiOH/PVA	1.6	0.911 F cm <sup>-2</sup>	0.324 mWh cm <sup>-2</sup>	16 mW cm <sup>-2</sup>	80% after 5000 at 20 mA cm <sup>-2</sup>	This work

## References

1. H. Gao, S. Cao and Y. Cao, *Electrochimica Acta*, 2017, **240**, 31-42.
2. K. Xu, W. Li, Q. Liu, B. Li, X. Liu, L. An, Z. Chen, R. Zou and J. Hu, *Journal of Materials*

- Chemistry A*, 2014, **2**, 4795.
3. J. Shen, X. Li, L. Wan, K. Liang, B. K. Tay, L. Kong and X. Yan, *ACS Applied Materials & Interfaces*, 2017, **9**, 668-676.
  4. X. Gong, S. Li and P. S. Lee, *Nanoscale*, 2017, **9**, 10794-10801.
  5. J. Sun, Y. Huang, C. Fu, Y. Huang, M. Zhu, X. Tao, C. Zhi and H. Hu, *J. Mater. Chem. A*, 2016, **4**, 14877-14883.
  6. Q. Zhang, X. Wang, Z. Pan, J. Sun, J. Zhao, J. Zhang, C. Zhang, L. Tang, J. Luo, B. Song, Z. Zhang, W. Lu, Q. Li, Y. Zhang and Y. Yao, *Nano Lett*, 2017, **17**, 2719-2726.
  7. B. Zheng, T. Huang, L. Kou, X. Zhao, K. Gopalsamy and C. Gao, *J. Mater. Chem. A*, 2014, **2**, 9736-9743.
  8. H. Xu, X. Hu, Y. Sun, H. Yang, X. Liu and Y. Huang, *Nano Research*, 2014, **8**, 1148-1158.
  9. W. Liu, N. Liu, Y. Shi, Y. Chen, C. Yang, J. Tao, S. Wang, Y. Wang, J. Su, L. Li and Y. Gao, *J. Mater. Chem. A*, 2015, **3**, 13461-13467.
  10. A. Sumboja, C. Y. Foo, X. Wang and P. S. Lee, *Adv Mater*, 2013, **25**, 2809-2815.
  11. X. Dong, Z. Guo, Y. Song, M. Hou, J. Wang, Y. Wang and Y. Xia, *Advanced Functional Materials*, 2014, **24**, 3405-3412.
  12. H. Xie, S. C. Tang, D. D. Li, S. Vongehr and X. K. Meng, *ChemSusChem*, 2017, **10**, 2301-2308.